

SESAR Engage KTN – PhD final report

PhD title:	STORMY: A pilot/dispatcher support tool based on the enhanced provision of thunderstorm forecast considering its inherent uncertainty
Candidate's name:	Eduardo Andrés Endériz
Lead supervisor's name:	Manuel Soler Arnedo
Co-supervisor's name (if applicable):	Maryam Kamgarpour
Proponent institute:	Universidad Carlos III de Madrid (UC3M)
Consortium institutes (if applicable):	ETH Zürich, Spanish Meteorological Office (AEMET), GTD Systems & Software Engineering
Thematic challenge:	TC3 Efficient provision and use of meteorological information in ATM
Edition date:	14 July 2022
Edition:	2.0
Dissemination level:	Public

The opinions expressed herein reflect the authors' views only. Under no circumstances shall the SESAR Joint Undertaking be responsible for any use that may be made of the information contained herein.



This project has received funding from the SESAR Joint Undertaking under the European Union's Horizon 2020 research and innovation programme under grant agreement No 783287.

Table of contents

Table of contents	2
List of Figures	3
1. Abstract	4
2. Objective of the study	4
3. Motivation	5
4. Advances this work has provided with regard to the state of the art	6
5. Methodology	6
6. Description of the data the study relies on	7
6.1. Scenario-Based RRT*	7
6.2. ARS for graph deformation	9
7. Computational experiments	10
7.1. Scenario-Based RRT*	10
7.2. ARS for graph deformation	11
8. Results	12
8.1. Scenario-Based RRT*	12
8.2. ARS for graph deformation	14
9. Analysis of the results	17
9.1. Scenario-Based RRT*	17
9.2. ARS for graph deformation	17
10. Conclusions and look ahead	18
11. References	19
11.1 Link to PhD thesis / repository	19
11.2 Associated outputs and publications	19
11.3 References cited in this report	20
Annex I: Acronyms	21

List of Figures

Figure 1. Methodology to build a probabilistic storm model based on RDT forecasts by means of a time-lagged ensemble forecast (see[5]).	8
Figure 2. Probability map (left), sample taken from it (center), and ensemble of 20 members (right).	9
Figure 3. Surface precipitation for 3 members of the EPS at intervals of 30 minutes. Initial date June 2nd, 2018, 13:00:00.	10
Figure 4. SB-RRT expansion (green) and solution (red) after 500, 1000 and 2000 iterations.	12
Figure 5. SB-RRT* expansion (green) and solution (red) after 500, 1000 and 2000 iterations.	12
Figure 6. Informed SB-RRT* expansion (green) and solution (red) after 500, 1000 and 2000 iterations.	13
Figure 7. Sensitivity of the SB-RRT* to the maximum number of iterations.	13
Figure 8. Sensitivity of the Informed SB-RRT* to the maximum number of iterations.	14
Figure 9. Cost of safety as a function of the number of iterations for the SB-RRT* and the Informed SB-RRT*.	14
Figure 10. Evolution of the solution with respect to time.	15
Figure 11. Trajectories sampled from the graph with respect to the numbers of iterations.	15
Figure 12. Estimated cost as a function of the number of iterations for 20 simulations.	16
Figure 13. Estimated fuel burn as a function of the estimated time of flight for different cost index.	16
Figure 14. Mach number and fuel consumption evolution as a function of ground distance from the origin for different cost index.	16

1. Abstract

Uncertainties inherent to convective weather constitute a major challenge for the Air Traffic Management System (ATM), affecting its safety, capacity, and efficiency. Specifically, thunderstorms represent an important threat, as they involve phenomena such as strong turbulence, wind shear or hail. It is essential to avoid them to ensure both passenger comfort and aircraft structural integrity. Thunderstorms' location and timing are hard to predict with certainty. This stochasticity is an important element that methodologies for aircraft trajectory planning must take into account.

For this purpose, two different methodologies for flight planning in areas of uncertain thunderstorm development are proposed. Both are heuristic approaches that rely on the iterative manipulation of graphs. Moreover, to enhance computational performance and enable real time operation, they are parallelized by means of GPU programming, producing results in less than seconds.

On one hand, the Scenario-Based Rapidly-Exploring Random Trees (Scenario-Based RRTs or SB-RRTs) are introduced, three algorithms for trajectory planning that explore an airspace with a tree structure. This kind of graph grows from the origin and looks for a connection with the destination through a safe sequence of tree branches. On the other hand, the Augmented Random Search (ARS) is proposed for trajectory deformation. This algorithm is applied to a graph, and it looks for the optimal sequence of edges, its relocation, and the best profile of velocities to minimize a combination of time and fuel.

The methodologies are tested with Ensemble Prediction Systems (EPS) that characterize atmospheric uncertainties through a set of possible forecasts. Results reveal that the algorithms are able to ensure safety and minimize objectives, such as time of flight, flight distance or fuel consumption.

2. Objective of the study

The objectives of this thesis are:

- Design of effective and efficient algorithms for aircraft trajectory planning and thunderstorm avoidance, since convective weather represents a major hazard for flights.
- The algorithms must incorporate Ensemble Prediction Systems (EPS). Thunderstorms are uncertain phenomena that require weather products of high spatiotemporal resolution to be captured. Although present EPS are not able yet, this will be achieved by future convective-permitting EPS. For this purpose, the designed algorithms must be compatible with EPS.

- From a computational perspective, algorithms must be efficient and return results in a fast manner (~ 10 seconds). Since the algorithms are to be used during the flight and thunderstorms evolve quickly, any methodology used for the planning must solve conflicts in near-real time.
- To validate the algorithms, they must be tested in realistic case studies. For this reason, EPS built on real weather data are used.

These objectives are aligned with Engage Thematic challenge 3: Efficient provision and use of meteorological information in ATM. The suggested methodologies will be compatible with high resolution weather products and will constitute possible support-tools for pilots and ATCOs.

3. Motivation

Uncertainties inherent to convective weather constitute a major challenge for the Air Traffic Management (ATM) system, affecting its safety, capacity and efficiency. For instance, in 2019 these phenomena accounted for a quarter of the en-route delays over Europe [1]. Specifically, thunderstorms represent an important threat, as they involve adverse events such as strong turbulence, wind shear and hail. Avoiding them is critical to guarantee both passengers' comfort and aircraft's structural integrity. Since flying in stormy regions is challenging for pilots, it often results in delayed and diverted flights, with the corresponding increase in operational costs. Additionally, thunderstorm prediction is a troublesome topic, and their inherent stochasticity must be accounted for by flight planning agents. The main motivation of this thesis is the design and implementation of algorithms for aircraft trajectory optimization constrained by uncertain regions of thunderstorm development to be used by pilots and ATCOs, thus reducing their workload for the sake of safety and efficiency.

It is worth noting that there are current efforts focused on the ground-air link of data with onboard information. The goal is to combine Numerical Weather Prediction (NWP) forecasts with radar, satellite and other additional observations, displaying the results on the cockpit [2]. Despite the fact that uplink systems have been successfully tested in the past in projects such as FLYSAFE [3] or eFlightOps [4], the real implementation in commercial aircraft is still under research. Aviation is subject to strict regulation and certification processes that need to be overcome before these systems are ready to be included in primary flight displays. However, the representation of such data on complementary devices (e.g., electronic flight bags) would provide pilots additional information and more time to react to thunderstorm evolution, minimizing deviations from the planned trajectory and hence saving fuel. An example of that type of technology is eWAS Pilot2, an app that provides pilots real time weather information from several sources through WiFi or 4G connections. Further motivation for this work would consist in designing methodologies to be integrated in the aforementioned systems, suggesting possible diversions from the flight plan to overcome updated weather events.

4. Advances this work has provided with regard to the state of the art

During the literature review, the identified research gap is the lack of algorithms for aircraft trajectory planning that account for uncertain thunderstorm development and achieve reduced computational times. On one hand, there are methodologies that successfully avoid uncertain storm cells, but are not computationally efficient to return fast results, e.g., [5, 6]. On the other hand, those tools that satisfy operational constraints do not work with stochastic weather data, e.g., [7-11].

On this basis, and from the objectives set in Section 2, two methodologies have been developed accordingly: the Scenario-Based RRT^{*1} and the Augmented Random Search for deformation of graphs (see Section 5). Both approaches meet the objectives:

- They are able to integrate EPS to characterize thunderstorm uncertainty in anticipation for future weather prediction products.
- They achieve computational times compatible with near-real time operation and produce results in less than 10 seconds.
- They are tested in case scenarios with data obtained from real weather data.

5. Methodology

For a given airspace X , the space of possible trajectories Γ is intractable, since there are multiple combinations of states s and controls u that would connect a pair of coordinates $x_0, x_f \in X$. For this purpose, the search is simplified. In this work, we consider a state space S that includes latitude ϕ , longitude λ , TAS v and mass m ; the control space U includes heading angles χ and thrust coefficient C_T .

Under these assumptions, there are two distinguishable pieces: First, a spatial component, represented by the evolution of latitude and longitude according to true heading. Second, a dynamic component, characterized by the evolution of TAS and mass due to thrust coefficient. These two fragments are modelled separately:

- The spatial component is approximated with a graph $G = \{A, E\}$, where $G \subset X$. The graph is formed by nodes $a \in A \subset X$ and edges $e \in E \subset X$. Each node is characterized by some particular coordinates included in the airspace $x \in X$, whereas each edge sets a connection between two nodes. For a given pair of nodes connected by an edge, the evolution of true heading is determined, and the integration of latitude and longitude is immediate.
- The dynamic component is defined with a Mach schedule M_s . The schedule represents the velocities that should be achieved when flying along any edge from the graph.

¹ Superscript * refers to the optimal variants of RRT algorithms. For compactness, RRT* is the Optimal RRT.

Since the changes in velocity are known, thrust T can be calculated from this variation, which also determines the evolution of mass.

This thesis presents two methodologies that make use of two different types of graph:

- The Rapidly-Exploring Random Tree (RRT) builds a tree that explores the safe space $X_{safe} \subset X$ (i.e., the space free of storms) through an iterative and random process. A tree is a particular kind of graph in which all the nodes are connected to an initial node by a sequence of edges. The goal of RRTs is to add the destination to the tree so that it is connected to the initial node with a safe path. If the process is successful, the algorithm returns a list of safe nodes and edges between origin and destination. In this work [a], the Scenario-Based RRT* (SB-RRT*) is presented, an optimal variant of RRTs that integrates EPS.
- The Augmented Random Search (ARS) algorithm is used to deform an initial graph [b]. In this case, the graph is built in a pre-processing stage and defines a set of multiple nodes and edges between origin and destination. The graph is created from a Voronoi diagram to set connections through regions that are less likely to be occupied by storms. The objective of the ARS is to find the most suitable sequence of nodes from a graph and relocate them to optimize a cost function.

6. Description of the data the study relies on

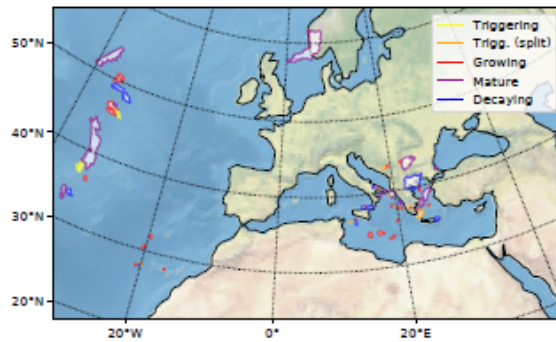
Different sources of information are considered for each of the methodologies:

6.1. Scenario-Based RRT*

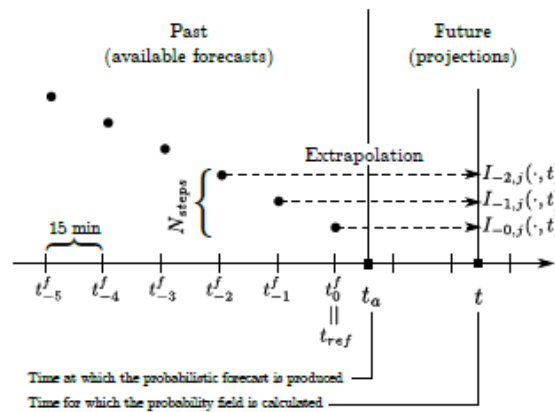
The test area consists of a stormy region detected by the Rapid Developing Thunderstorms (RDT) (<http://www.nwcsaf.org/web/guest/nwc/geo-geostationary-near-real-time-v2018>) system on November 16th, 2017 at 6:00 Zulu time. RDT is a product developed by Meteo-France for the detection, monitoring and forecast of convective cells, which uses imagery obtained by Meteosat Second Generation satellites. It is able to characterize convective systems around Europe every 15 minutes with a horizontal resolution of 3 km.

RDT output includes a list of convective objects (Fig. 1(a)), as well as their speed, direction of motion, phase (e.g. growing, decaying.) and a deterministic extrapolation into the future. This data is post-processed, as illustrated in Fig. 1(b), incorporating uncertainties in the cell motion and obtaining the probability map $p(x)$ shown in Fig. 1(c). The function p represents the probability that $x \in X$ is in a storm, where $x = (\phi, \lambda)$. To be able to capture storm cells more accurately, NWP is evolving towards convective-permitting ensemble prediction systems (EPS) of very high spatiotemporal resolution. These are not available yet but are expected in the near future. In consequence, to simulate an ensemble-based input and obtain different possible forecasts for the SB-RRTs, different ensemble members are sampled from the probability map in Fig. 2(a) as follows:

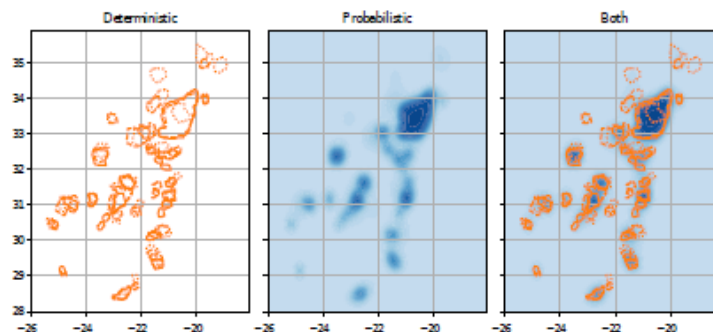
- The map is first discretized with a 0.1 deg step in latitude and longitude.
- For each position, a random number is taken from a uniform distribution between 0 and 1. If this number is lower than the actual probability of storm at the position, a storm is assigned to that position. For example, if the probability of having a storm is 90%, any sample between 0 and 0.9 corresponds to having a storm.
- The positions with a storm are clustered by means of a density-based clustering method, DBSCAN [12]. Finally, the polygon that encloses each cluster is calculated [13].



(a) Example of convective systems identified by RDT.



(b) Time-lagged ensemble methodology.



(c) Probabilistic storm model compared to the deterministic RDT data.

Figure 1. Methodology to build a probabilistic storm model based on RDT forecasts by means of a time-lagged ensemble forecast (see[5]).

An example of the process is shown in Fig. 2(b). As the result is a group of polygons, the intersection of each polygon with a RRT edge, if it exists, can be calculated by means of geometric operations. Fig. 2(c) shows an example with 20 ensemble members.

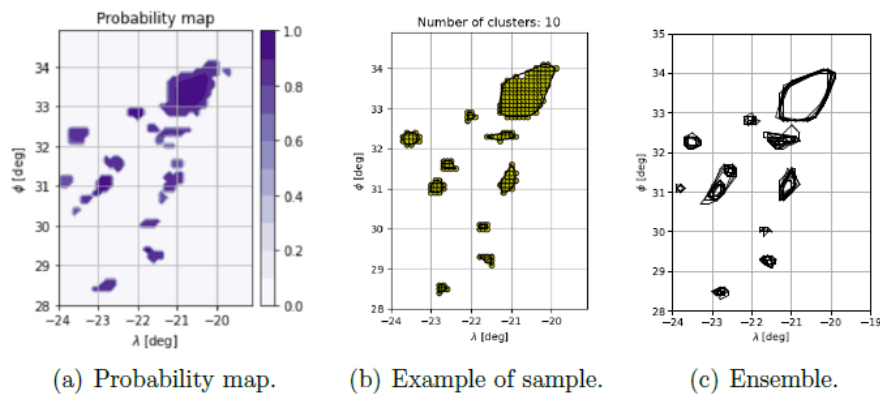


Figure 2. Probability map (left), sample taken from it (center), and ensemble of 20 members (right).

6.2. ARS for graph deformation

The ARS algorithm is being used to deform a graph that, for example, can represent a structured airspace. The objectives of such deformations are twofold: First, minimize costs and reduce flight times. Second, adapt to any possible motion in the storm cells. For this purpose, this section covers how a time varying ensemble forecast was obtained. To produce a precipitation nowcast, the open source library Pysteps [14] has been used. Pysteps provides a modular framework for researchers interested in developing new methods for nowcasting and stochastic simulation of precipitation. It is a highly configurable and easily accessible platform suitable for researchers ranging from weather forecasters to hydrologists. The Pysteps library implements several optical flow methods as well as advanced stochastic generators to produce ensemble nowcasts.

In this work, OPERA [15] radar images are used as the observational input for Pysteps. OPERA is the EUMETNET (<https://www.eumetnet.eu/>) operational weather radar network in Europe that covers more than 30 countries and contains more than 200 weather radars. OPERA produces three types of composites: instantaneous surface rain rate, instantaneous maximum reflectivity and hourly rainfall accumulation. These composites cover the whole of Europe in a Lambert Equal Area projection and they are updated every 15 minutes.

- In the rain rate composite each composite pixel is a weighted average of the valid pixels of the contributing radars, weighted by a quality index, the distance from center of the pixel and an exponential index related to inverse of the beam altitude.
- The rainfall accumulation composite is simply the sum of the previous four 15-minute rain-rate products.
- In the maximum reflectivity composite each composite pixel contains the maximum of all polar cell values of the contributing radars at that location.

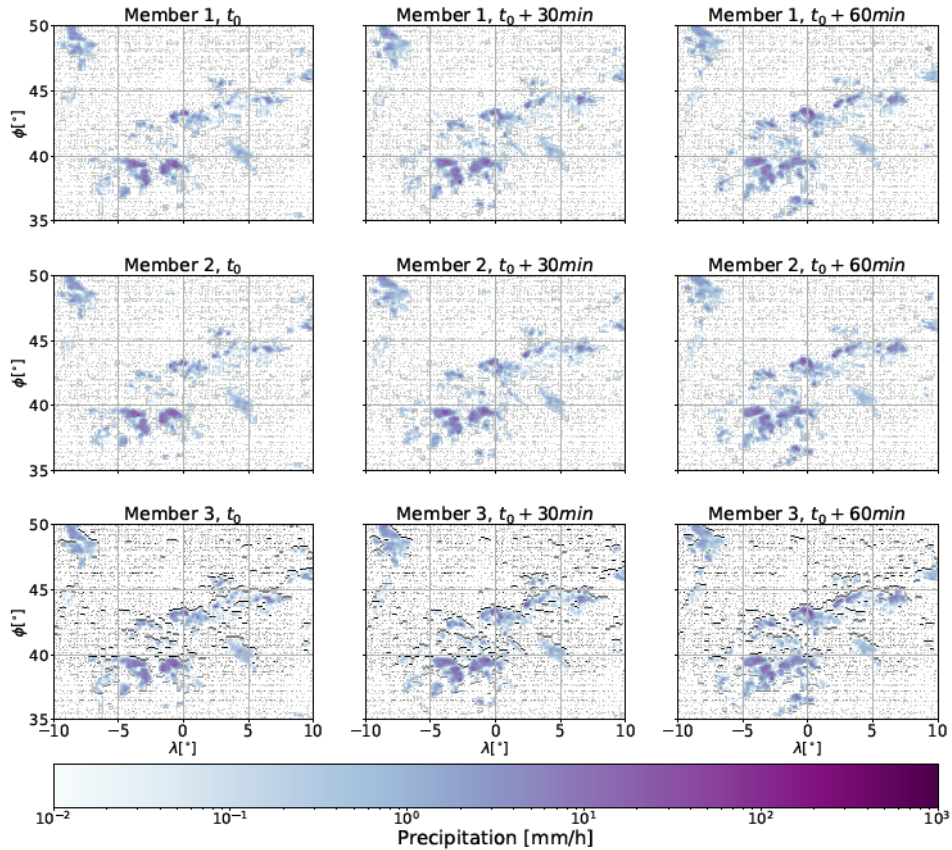


Figure 3. Surface precipitation for 3 members of the EPS at intervals of 30 minutes. Initial date June 2nd, 2018, 13:00:00.

Then, nowcast are produced by the following steps. First, the optical flow Lucas-Kanade [16] algorithm is applied to two consecutive rain rate composites for finding an estimation of the precipitation motion field. Secondly, the motion field is used to generate a deterministic nowcast with the S-PROG model [17]. The S-PROG algorithm implements a scale filtering approach in order to progressively remove the unpredictable spatial scales during the forecast. Finally, an stochastic component is added to the deterministic forecast using the STEPS method [18]. The result is an ensemble of 15 nowcast of the precipitation field. A sample of 3 members of the ensemble is shown in Fig. 3, at intervals of 30 minutes, starting at 13:00:00 on June 2nd, 2018.

7. Computational experiments

7.1. Scenario-Based RRT*

Three algorithms were tested in [a]:

- SB-RRT: an update of RRT that integrates EPS and guarantees safety up to a user-defined safety margin ϵ . This algorithm only ensures safety and do not lead to optimal solutions. Each time the algorithm runs, it returns a completely different and random trajectory.

- SB-RRT*: a variant of SB-RRT that ensures safety and asymptotic optimality. It includes routines that reorganize the internal structure of the tree to minimize the distance between the origin and any other coordinate (such as the destination).
- Informed SB-RRT*: a variant of SB-RRT* that enhances convergence. Since the SB-RRT* does not converge efficiently, the search is focused on the regions around the optimal solution, and not all the airspace.

The algorithms and their pseudocodes are presented and detailed in [a]. The novelty of these approaches is the so-called dynamic risk allocation that ensures safety under uncertainties captured by EPS. The algorithms are tested using a kinematic model of an aircraft at constant altitude and airspeed. Note that they would be able to handle more complex dynamical models, but the goal of this work was to demonstrate how to deal with ensemble-based weather products.

The methodologies require calculating the intersections between each branch of the tree and a set of polygons. This repetitive task is implemented in parallel, through GPU computations. As a consequence, simulations were sped up from days to seconds. Computational times, were reduced by a factor between 500 and 5000 depending on the number of members in the ensemble

In the case study included in [a], the state variables are latitude and longitude, and the airspace is $[-24^\circ, -19^\circ] \times [28^\circ, 35^\circ]$. The aircraft flies between $(-22^\circ, 34^\circ)$ and $(-20^\circ, 29^\circ)$ at constant flight level FL300. The weather data is obtained according to the process in section 6.1, getting an ensemble of 20 members. The computations were performed in a workstation equipped with an Intel Xeon E3-1240 CPU running at 3.5 GHz and a NVIDIA Quadro M4000 GPU of 8 GB.

7.2. ARS for graph deformation

A new methodology for trajectory deformation is presented and tested in [b]. To this end, a graph between origin and destination is created, setting multiple possible connections between them. With the Augmented Random Search (ARS) algorithm, we address two objectives:

- Find a sequence of edges in the graph that connect origin and destination.
- Relocate and deform those edges and find a velocity schedule that allows to reduce time of flight, fuel consumption, and avoid moving storms.

An optimization problem is formulated, in which the objective function is a weighted combination of total time of flight, fuel consumption and time spent in storms. Such objective is minimized in average accounting for the effects of all the members in the EPS. By tuning the weight corresponding to each objective, different goals are achieved: minimum time of flight, minimum consumption, no risk of storms.

In the case study included in [b], the state variables are latitude, longitude, TAS and mass, and the airspace is $[35^\circ, 50^\circ] \times [-15^\circ, 15^\circ]$. The aircraft flies between $(47^\circ, 5^\circ)$ and $(38^\circ, -5^\circ)$ at constant flight level FL300. The BADA model for A320 is considered for the aerodynamic and propulsive forces. The weather data ensemble in section 6.1, with an ensemble of 15 members. The computations were performed in a workstation equipped with an Intel Xeon E3-1240 CPU running at 3.5 GHz and a NVIDIA Quadro M4000 GPU of 8 GB.

8. Results

8.1. Scenario-Based RRT*

All the graphs in this section are published in [a]. First, the growth of each of the three variants of RRT is presented, for 500, 1000 and 2000 iterations. In Fig. 4, the expansion of the SB-RRT is shown. This algorithm is not optimal, and every simulation produces a different random and safe solution.

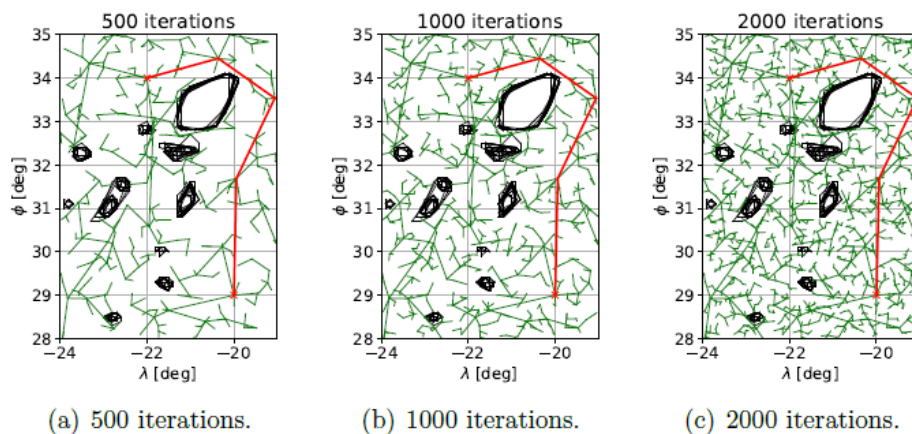


Figure 4. SB-RRT expansion (green) and solution (red) after 500, 1000 and 2000 iterations.

Fig. 5 shows the expansion of a SB-RRT*. The tree grows occupying the safe space and minimizing the flight distance to each coordinate.

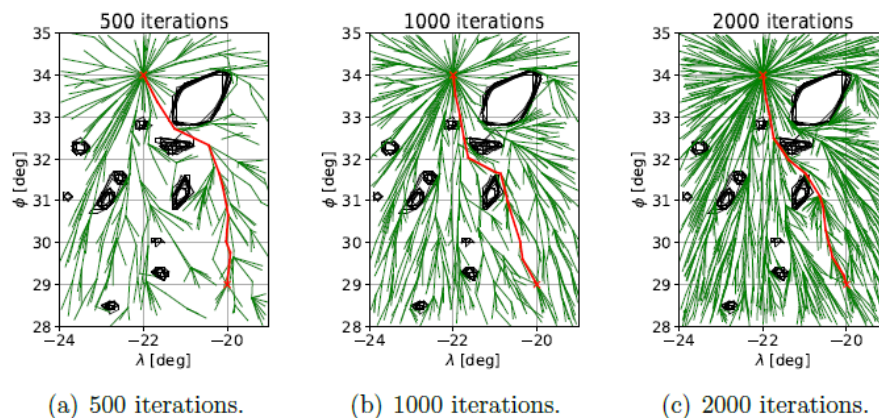


Figure 5. SB-RRT* expansion (green) and solution (red) after 500, 1000 and 2000 iterations.

To conclude, the growth of Informed SB-RRT* is shown in Fig. 6. The search is limited to the region around the solution of minimum cost. It starts growing as a SB-RRT*, but once a solution is found, the search is narrowed to an ellipsoid. This ellipsoid shrinks when a better solution is obtained.

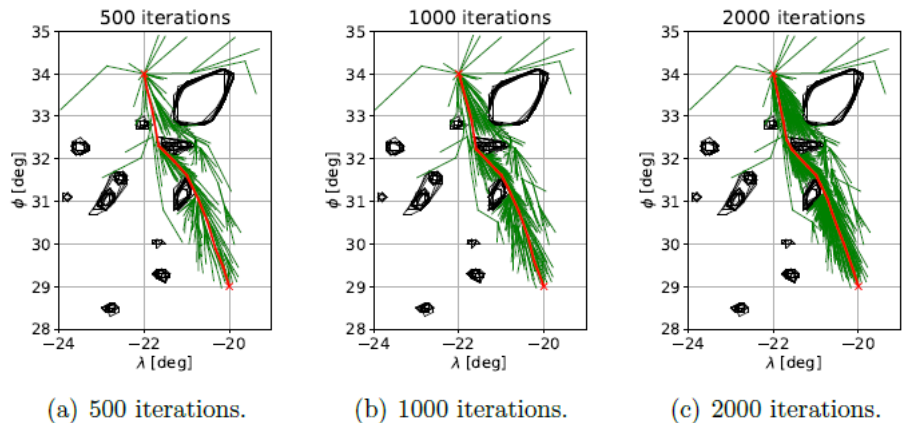


Figure 6. Informed SB-RRT* expansion (green) and solution (red) after 500, 1000 and 2000 iterations.

Since the RRT is a heuristic methodology that grows randomly, the sensitivity of the three variants is shown. First, the SB-RRT* is presented in Fig. 7. Three different local solutions are obtained. Contrariwise, the informed variant is able to go directly to the optimum in less iterations as shown in Fig. 8.

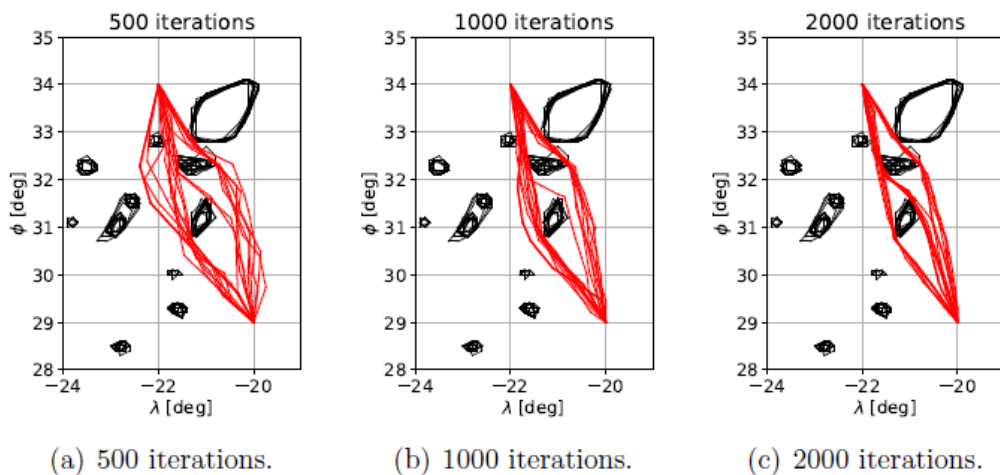


Figure 7. Sensitivity of the SB-RRT* to the maximum number of iterations.

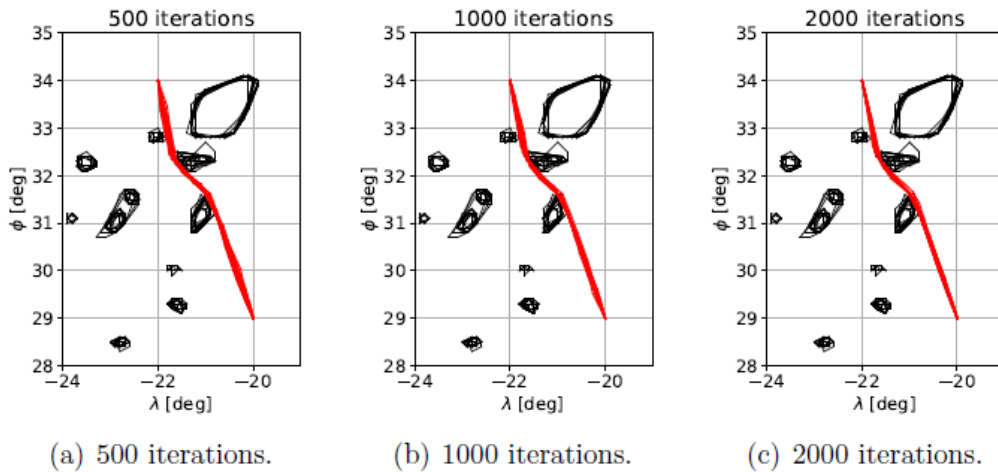


Figure 8. Sensitivity of the Informed SB-RRT* to the maximum number of iterations.

To conclude, the evolution of cost with the number of iterations for multiple simulations is shown in Fig. 9. The difference in flight distance with respect to the great circle connecting origin and destination (cost of safety) is plotted. Different colour bands represent 0, 10, 90, 100 percentiles, whereas the solid black line is the median.

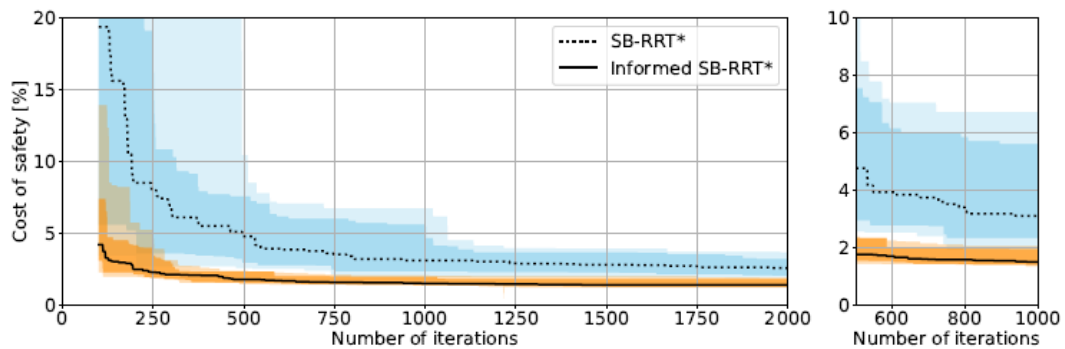


Figure 9. Cost of safety as a function of the number of iterations for the SB-RRT* and the Informed SB-RRT*.

8.2. ARS for graph deformation

All the graphs in this section are under review for publication in [b]. First, the trajectory obtained as a solution in the case study is shown in Fig. 10. Second, Fig. 11 shows the trajectories that are sampled from the graph during the iterative process in the ARS. In the beginning, the samples cover the entire graph, however, as the algorithm converges, the optimal trajectory is sampled with probability 1.

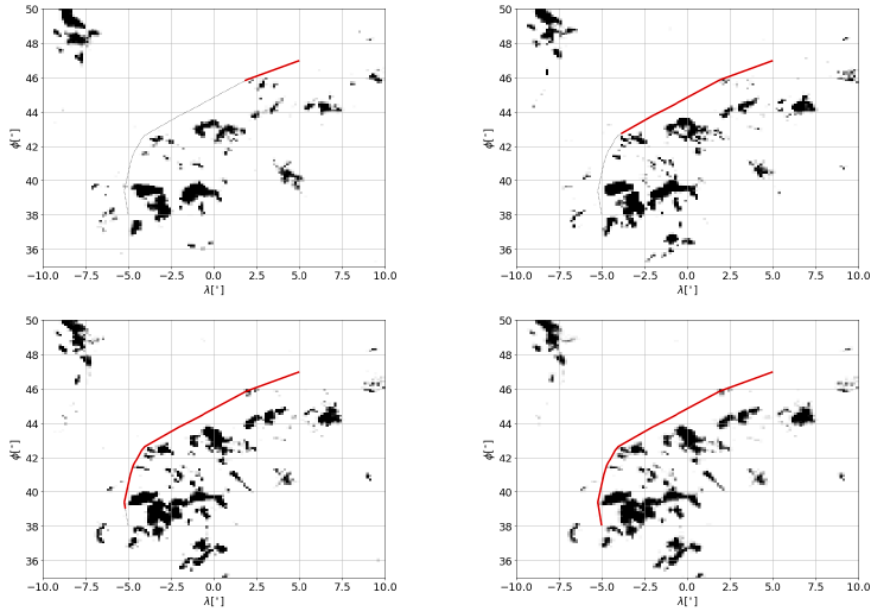


Figure 10. Evolution of the solution with respect to time.

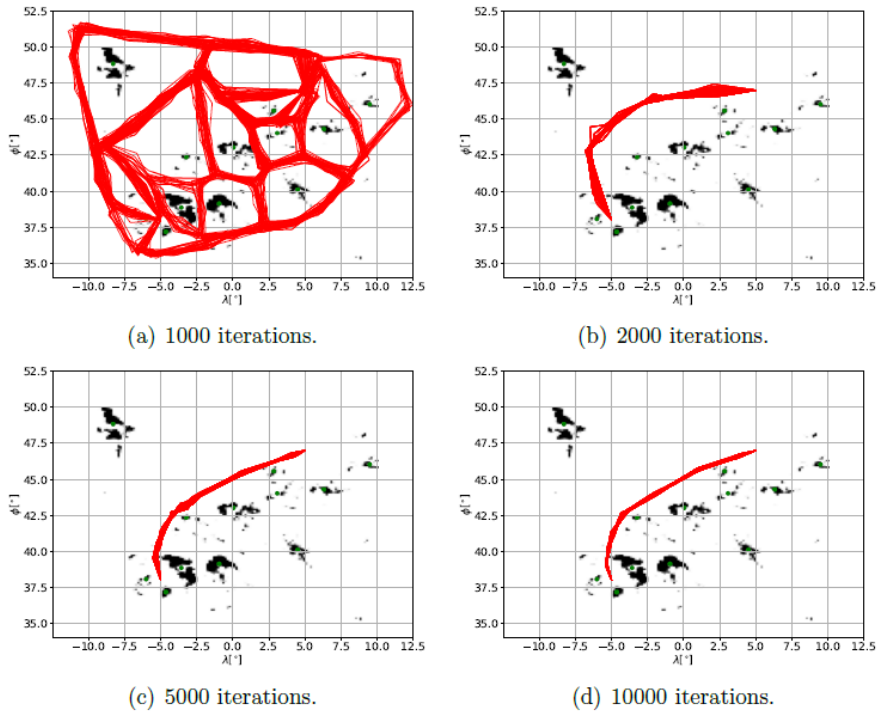


Figure 11. Trajectories sampled from the graph with respect to the numbers of iterations.

Since the ARS is a heuristic algorithm, the objective function converges in a different manner during each simulation. The evolution of cost with respect to the number of iterations is shown in Fig. 12 for 20 simulations. Different colour bands represent 0, 10, 90, 100 percentiles, whereas the solid black line is the median.

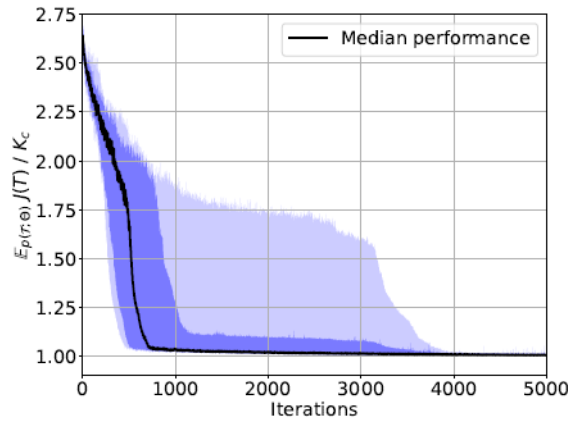


Figure 12. Estimated cost as a function of the number of iterations for 20 simulations.

To conclude, the effects of a cost index (time/fuel) in the state variables are shown in the Pareto frontier from Fig. 13 and the profiles from Fig. 14.

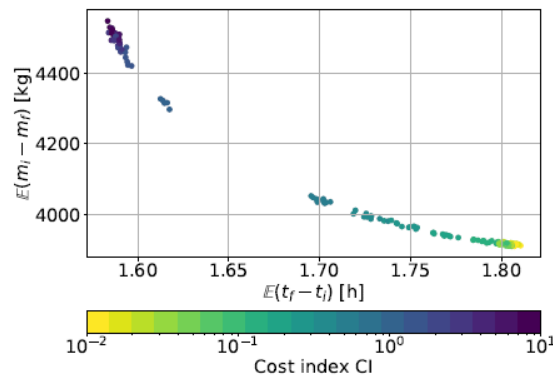
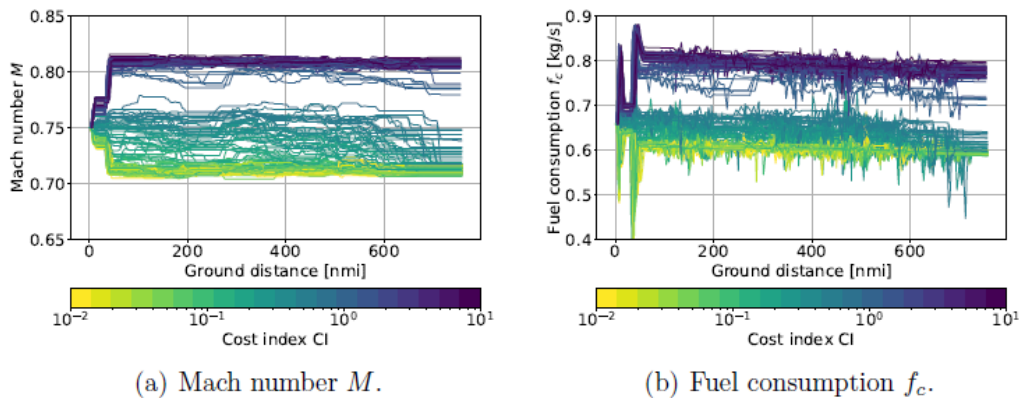


Figure 13. Estimated fuel burn as a function of the estimated time of flight for different cost index.



(a) Mach number M .

(b) Fuel consumption f_c .

Figure 14. Mach number and fuel consumption evolution as a function of ground distance from the origin for different cost index.

During a research stay at EPFL (Dec21-Mar22), the second approach was extended to consider multiple aircraft. The result is a methodology that can be used to avoid storms and conflicts between aircraft. A conference paper that details this variation was submitted [e].

9. Analysis of the results

9.1. Scenario-Based RRT*

The analysis of the SB-RRT* results reveals that during the first series of iterations (Figs. 7(a)-7(b)) there is a wide spectrum of safe solutions, but none of them are optimal. As the iterations increase (Fig. 7(c)), it is noticeable that the algorithm converges to 3 possible solutions, thus indicating the existence of different local optima. This is indeed a positive fact, as different alternatives, all of them safe, can be proposed to both pilots and air traffic controllers in times compatible with practical settings (seconds/minutes). Contrariwise, the trajectories provided by the Informed SB-RRT* converged to the global optimum (in terms of flight distance) after a lower number of iterations (Figs. 8(a)-8(c)). All the SB-RRT* simulations would eventually converge to this same solution but involving a larger number of iterations. This fact demonstrates the higher efficiency of the informed approach.

To conclude, a percentile representation of the cost function is shown in Fig. 9 for 20 simulations, considering the SB-RRT* and the Informed SB-RRT*. The region of interest between 500 and 1000 iterations is zoomed on the right. It can be observed that as the maximum number of iterations is increased, the cost of safety decreases, and so does the variability in the solutions. These results allow the conclusion that it might not be necessary to run the algorithms for a large number of iterations. On one hand, the highest costs obtained by the SB-RRT* after 500 and 1000 iterations were 10.4% and 6.7%, respectively. In half of the simulations, the error is less than 4.7% and 3.1% after 500 and 1000 iterations, respectively. On the other hand, as was to be expected, the Informed SB-RRT* presented less variability for the same number of iterations. The highest costs were 2.4% and 2.0% after 500 and 1000 iterations, respectively.

Although the SB-RRT* is a slightly faster algorithm, it requires more iterations to reach the same convergence levels. By way of example, the 300 iterations of the Informed SB-RRT* take 10 seconds, whereas running the SB-RRT* for 1000 iterations takes around 1 minute.

9.2. ARS for graph deformation

The maximum number of iterations represents the stopping criteria for the algorithm. It is required to be large enough to ensure convergence to a close-to-optimum solution, but not too large to ensure computational times are compatible with near real time operation. Fig.11 represents the population of paths sampled from the graph. There are three phases that can be observed (and were present in all the simulations):

- Exploration: After 1000 iterations (Fig. 11(a)), the population is covering the entire initial graph with some slight deformations. During this phase, the algorithm is mainly optimizing the successor choice, testing a wide variety of paths and checking which of them are more efficient

- Offset regulation: Then, after 2000 iterations (Fig. 11(b)), the algorithm has found which sequence of nodes is more convenient, starts looking for the optimal offsets and adapts to weather features. It can be observed that the population is condensed around a main path.
- Finally, after 5000 to 10000 iterations (Figs.11(c)-11(d)), the Mach schedule is refined to meet with the cost function requirements (fast trajectory vs fuel savings).

ARS is a heuristic algorithm that explores a parametric space based on a randomized process to reach an optimal solution. For each simulation, the search is performed in a different manner. Ideally, the algorithm would be running indefinitely, always looking for slight drops in cost. However, since that is impossible, the smallest number of iterations that produces results with a reduced variability is sought. It is expected that during the first iterations the cost evolution varies between simulations, but after a sufficient number of them, the results should converge to the same values. To show this variability, the evolution of expected cost with respect to the number of iterations is shown in Fig. 12 considering 20 simulations. As it was expected during ~4000 iterations, there exists a variability in the results between simulations. However, after a larger number, these differences are negligible. In consequence, after ~4000 iterations and a computational time of ~8 seconds, the algorithm has converged producing the close-to-optimal solutions included in Fig. 10.

To conclude, the effects of the cost index are analysed. As it was expected, for a lower cost index, the algorithm minimizes fuel, reducing consumption and velocity, leading to large time of flight. On the contrary, a large cost index implies flying faster, increasing fuel consumption and reducing total time. This is shown in Figs. 9-10.

10. Conclusions and look ahead

In this thesis, two different methodologies for aircraft trajectory optimization under uncertain thunderstorm development are presented. In anticipation of future NWP products, an ensemble of possible weather forecasts is used to characterize these uncertainties. Moreover, both works rely on parallel GPU programming, producing close-to-optimum solutions in seconds and being compatible with near-real time operation.

In first place, the scenario-based methodology for RRTs is detailed and applied to the RRT, the RRT* and the Informed RRT*. This leads to the so-called Scenario-Based RRTs, three algorithms for flight planning in areas of convective weather. Each of them is able to find a safe trajectory between a pair origin-destination constrained with a safety margin. Additionally, the SB-RRT* and the Informed SB-RRT* are used to minimize flight distance and increase efficiency. Secondly, an algorithm for graph deformation based on the Augmented Random Search is proposed. The result is a code for aircraft trajectory planning able to connect two states with a safe trajectory. Given a relative weight between time of flight and fuel consumption, it finds the most efficient route.

The main disadvantage of heuristic techniques such as RRTs or ARS is that each iterative process and the convergence towards a solution is different. For this purpose, a sensitivity analysis is performed, revealing that the algorithms require less than 10 second to converge.

As follow-up activities, the effect of the number of storm cells and their arrangement on the convergence rate will be explored, as the number of iterations to approach close-to-optimum solutions seems to be affected. The geographical region might also be considered in the analysis, since weather changes notably between them. Additionally, the formulation can be extended to consider not only weather but restricted areas or congested sectors.

11. References

11.1 Link to PhD thesis / repository

Eduardo is finalizing the writing of the PhD Thesis. Expected defence in October-November 2022.

His profile can be checked <https://uc3m-phd-aerospace.es/portfolio/eduardo-andres/>

The PhD thesis will be made available in his profile as soon as it is defended.

11.2 Associated outputs and publications

Journal papers:

- *[a] Informed Scenario-Based RRT* for Aircraft Trajectory Planning under Ensemble Forecasting of Thunderstorms.* E. Andrés, D. González-Arribas, M. Soler, M. Kamgarpour, M.Sanjurjo-Rivo. Transportation Research Part C, 2021. <https://doi.org/10.1016/j.trc.2021.103232>
- *[b] Iterative Graph Deformation for Aircraft Trajectory Planning Considering Ensemble Forecasting of Thunderstorm.* E. Andrés, D. González-Arribas, M. Soler, M. Kamgarpour, M. Sanjurjo-Rivo. (Under review, Submitted to Transportation Research Part C).

Conference papers:

- *[c] GPU-Accelerated RRT for Flight Planning Considering Ensemble Forecasting of Thunderstorms.* E. Andrés, D. González-Arribas, M. Sanjurjo-Rivo, M.Soler, M. Kamgarpour. SESAR Innovation Days 2020.
- *[d] Scenario Based RRT* for Aircraft Trajectory Planning under Uncertain Thunderstorm Development.* E. Andrés, D. González-Arribas, M. Sanjurjo-Rivo, M. Kamgarpour, and M. Soler. ENRI International Workshop on. ATM/CNS (EIWAC) 2019, Tokio.
- *[e] Multi-Aircraft Trajectory Deformation for Uncertain Thunderstorm Avoidance and Conflict Resolution.* E. Andrés, M. Soler, T. A. Wood, M. Kamgarpour, M. Sanjurjo-Rivo and J. Simarro. (To be accepted, submitted to International Workshop on. ATM/CNS (IWAC) 2022, Tokyo).

Book chapters:

- [f] *RRT*-Based Algorithm for Trajectory Planning Considering Probabilistic Weather Forecasts*. E. Andrés, M. Kamgarpour, M. Soler, M. Sanjurjo-Rivo, D. González-Arribas. *Air Traffic Management and Systems IV*. Springer, 2021. 10.1007/978-981-33-4669-7

11.3 References cited in this report

[1] Eurocontrol. Performance Review Report. An Assessment of Air Traffic Management in Europe during the Calendar Year 2019. Tech. rep. 2020.

[2] C. Forster et al. “Satellite-Based Real-Time Thunderstorm Nowcasting for Strategic Flight Planning En Route”. In: *Journal of Air Transportation* 24.4 (2016), pp. 113–124.

DOI: 10.2514/1.D0055.

[3] R W. Lunnon et al. “FLYSAFE Meteorological Hazard Nowcasting Driven by the Needs of the Pilot”. In: American Meteorological Society. Sept. 2009.

URL: <https://ams.confex.com/ams/pdfpapers/103462.pdf>.

[4] C. Kessinger et al. “Demonstration of a Convective Weather Product into the Flight Deck”. In: American Meteorological Society. Feb. 2015.

URL: <https://ams.confex.com/ams/95Annual/webprogram/Paper269015.html>.

[5] D. González-Arribas et al. “Robust Aircraft Trajectory Planning Under Uncertain Convective Environments with Optimal Control and Rapidly Developing Thunderstorms”. In: *Aerospace Science and Technology* 89 (2019), pp. 445–459. DOI: 10.1016/j.ast.2019.03.051.

[6] D. Hentzen et al. “On Maximizing Safety in Stochastic Aircraft Trajectory Planning with Uncertain Thunderstorm Development”. In: *Aerospace Science and Technology* 79 (2018), pp. 543–553. URL: <https://doi.org/10.1016/j.ast.2018.06.006>.

[7] K. S. Sheth et al. *Air Traffic Management Technology Demonstration - 3 (ATD-3). Operational Concept for the Integration of ATD-3 Capabilities*. Tech. rep. National Aeronautics and Space Administration, 2018.

[8] J. Henderson. *The Traffic Aware Strategic Aircrew Requests (TASAR) Concept of Operations*. Tech. rep. Engility Corporation for the National Aeronautics and Space Administration, 2013.

[9] D. McNally et al. “Dynamic Weather Routes: Two Years of Operational Testing at American Airlines”. In: *Air Traffic Control Quarterly* 23.1 (2015), pp. 55– 81.

DOI: 10.2514/atcq.23.1.55. URL: <https://doi.org/10.2514/atcq.23.1.55>.

[10] D. Isaacson and C. Gong. Dynamic Routes for Arrivals in Weather (DRAW) Concept of Operations. Tech. rep. National Aeronautics and Space Administration, 2018.

[11] C. Gong and D. McNally. “Dynamic Arrival Routes: A Trajectory-Based Weather Avoidance System for Merging Arrivals and Metering”. In: 15th AIAA Aviation Technology, Integration and Operations Conference. 2015. DOI: 10.2514/6.2015-3394.

[12] P. Kroger, S. Jorg, A. Zimek, “Density-based clustering”, WIREs Data Mining Knowl Discov (2011). URL <https://doi.org/10.1002/widm.30>.

[13] F. P. Preparata, S. J. Hong, “Convex hulls of finite sets of points in two and three dimensions”, Communications of the ACM (1977).

[14] A. Huuskonen, E. Saltikoff, I. Holleman, “The operational weather radar network in Europe”, Bulletin of the American Meteorological Society 95 (6) (2014) 897 – 907. doi:10.1175/BAMS-D-12-00216.1.

[15] J. Y. Bouguet, “Pyramidal implementation of the Lucas Kanade feature tracker”, Intel Corporation, Microprocessor Research Labs (2001).

[16] A. W. Seed, “A dynamic and spatial scaling approach to advection Forecasting”, Journal of Applied Meteorology 42 (3) (2003) 381 – 388.

[17] A. W. Seed, C. E. Pierce, K. Norman, “Formulation and evaluation of a scale decomposition-based stochastic precipitation nowcast scheme”, Water Resources Research 49 (10) (2013) 6624–6641. doi: <https://doi.org/10.1002/wrcr.20536>.

Annex I: Acronyms

Term	Definition
ARS	Augmented Random Search
ATM	Air Traffic Management
EPS	Ensemble Prediction System
NWP	Numerical Weather Prediction
RRT	Rapidly-Exploring Random Tree
TAS	True Airspeed